Journal of Magnetic Resonance 197 (2009) 208–212

Contents lists available at ScienceDirect

Journal of Magnetic Resonance

journal homepage: www.elsevier.com/locate/jmr

Application of low field NMR T_2 measurements to clathrate hydrates

Shuqiang Gao [a,*], Walter G. Chapman [a], Waylon House [b]

[a] Chemical Engineering Department, Rice University, 6100 Main St., Houston, TX 77251, USA
[b] Petroleum Engineering Department, Texas Tech University, Lubbock, TX 79406, USA

ARTICLE INFO

Article history:
Received 9 July 2008
Revised 25 December 2008
Available online 13 January 2009

Keywords:
T_2 distribution
THF
Mechanism
Gas hydrate
Water structure
Deuterium oxide
NMR

ABSTRACT

Low field (2 MHz) Nuclear Magnetic Resonance (NMR) proton spin–spin relaxation time (T_2) distribution measurements were employed to investigate tetrahydrofuran (THF)—deuterium oxide (D_2O) clathrate hydrate formation and dissociation processes. In particular, T_2 distributions were obtained at the point of hydrate phase transition as a function of the co-existing solid/liquid ratios. Because T_2 of the target molecules reflect the structural arrangements of the molecules surrounding them, T_2 changes of THF in D_2O during hydrate formation and dissociation should yield insights into the hydrate mechanisms on a molecular level. This work demonstrated that such T_2 measurements could easily distinguish THF in the solid hydrate phase from THF in the coexisting liquid phase. To our knowledge, this is the first time that T_2 of guest molecules in hydrate cages has been measured using this low frequency NMR T_2 distribution technique. At this low frequency, results also proved that the technique can accurately capture the percentages of THF molecules residing in the solid and liquid phases and quantify the hydrate conversion progress. Therefore, an extension of this technique can be applied to measure hydrate kinetics. It was found that T_2 of THF in the liquid phase changed as hydrate formation/dissociation progressed, implying that the presence of solid hydrate influenced the coexisting fluid structure. The rotational activation measured from the proton response of THF in the hydrate phase was 31 KJ/mole, which agreed with values reported in the literature.

1. Introduction

Gas hydrates, also known as clathrate hydrates, are ice-like compounds in which water molecules, under high pressures and low temperatures, form structures composed of nano-scale polyhedral cages that host small guest molecules such as methane and ethane [1]. The importance of gas hydrates has been realized in many areas, including flow assurance [2], global climate models [3], and potential future energy resources [4]. However, the knowledge of molecular mechanisms of hydrate formation/dissociation has been proven to be one of the continuing puzzles of physical chemistry despite enormous prior research efforts devoted to this subject [5–18]. Understanding at this fundamental level has been hindered mainly by the lack of experimental tools that are capable of directly observing the hydrate phase and sensitive enough to detect rapidly changing molecular motions and environments.

Low frequency NMR spin–spin relaxation time (T_2) distributions have been routinely applied in the petroleum industry to characterize rock matrix and measure downhole fluid properties [19]. Although many NMR studies on gas hydrates have been reported in the literature [20–23], most of those works focused on the solid phase at low temperatures and high frequencies where the long correlation time limit applies. Low field NMR techniques have rarely been used for hydrate studies because of the lower signal to noise ratio and because it was unclear that encaged molecules would exhibit motional narrowing—even at these low fields. An attempt by Schlumberger [24] to measure T_2 distributions in methane hydrate using a 2 MHz Resonance Instruments (RI) Maran spectrometer failed in obtaining methane T_2 data in the hydrate cages. Garg et al. [25] reported the proton line widths of THF in D_2O hydrate at various temperatures, which were measured by wide-line spectroscopy at 16 MHz. It was suggested that THF molecules undergo rapid isotropic rotations in D_2O clathrate cages. Assuming Gaussian lineshapes, this data would indicate T_2's of about 0.5 ms for THF at 207 K, which should be long enough to be measurable by a 2 MHz RI Maran spectrometer that has receiver dead time of 60 μs. Since T_2 is an indicator of the local molecular ordering around the spin-bearing molecules, the T_2 distributions of THF in D_2O during hydrate transitions should provide a new way of gathering information regarding hydrate molecular mechanisms.

In this work, proton NMR T_2 distribution measurements were used to monitor THF/D_2O hydrate formation and dissociation processes. THF forms Structure II hydrate [25,26] and THF molecules

* Corresponding author. Present address: Shell Global Solutions, USA. Fax: +1 281 544 8826.
E-mail address: sqgao@alumni.rice.edu (S. Gao).

1090-7807/$ - see front matter © 2009 Elsevier Inc. All rights reserved.
doi:10.1016/j.jmr.2008.12.022

occupy only the large clathrate cages in the solid hydrate lattice. Results demonstrated that the T_2 distribution of THF molecules in D_2O clathrate cages can be fully captured with a 2 MHz RI Maran coincidently with the T_2 distribution of THF molecules within a coexisting liquid phase. To our knowledge, this is the first time that the 2 MHz NMR T_2 distribution technique has been successfully applied to study gas hydrates. The influence of a hydrate phase on the coexisting fluid structure [27] was also suggested by the change in T_2 of THF in the liquid phase as the solid to liquid ratio changed at the hydrate equilibrium temperature. Since the area under the proton T_2 distribution of the hydrate phase represents the population of the enclathrated THF molecules, an extension of this technique can provide information on intrinsic hydrate kinetics.

2. Experimental

The schematic of the experimental setup was shown in Fig. 1. D_2O was chosen instead of H_2O to form hydrate with THF because D_2O does not respond to proton NMR and therefore the proton response of THF can be studied without interference. HPLC Grade THF (99.97%) was obtained from Sigma–Aldrich in inhibitor free form and it was supplied under a nitrogen atmosphere. T_2 measurements of the protons in THF in D_2O (Cambridge Isotope Laboratories, D 99.9%) were obtained with a 2 MHz RI Maran NMR spectrometer using Carr–Purcell–Meiboom–Gill (CPMG) technique. This instrument has a receiver dead time of 60 μs. Data were acquired using the *RiNMR* software and processed using the *WinDXP* program.

The temperature of the spectrometer has to be kept constant at 30 °C to maintain the stability of the system's permanent magnet. Therefore, a thermal insulation material was placed along the inside surface of the sample bore as an Air-Jet temperature controller-supplied dry air to control the sample temperature. This controller is capable of providing air temperature from −40 to 100 °C with 0.1 °C stability. A glass bottle with a cap that has a Teflon liner was used to contain 20 ml of THF–D_2O solution (molar ratio 1:17) and was tightly sealed to prevent THF evaporating into the environment. The sample was weighed and no THF loss was detected after two weeks. A LUXTRON fluoroptic thermometer was mounted into the glass container through the cap to monitor the sample temperature with a resolution of 0.1 °C. A dummy experiment was performed with everything in place but no THF–D_2O in the sample bottle to make sure that there was no unwanted proton signal.

Since trace amounts of oxygen may alter the T_2 of THF significantly, pure D_2O and THF liquids were deoxygenated separately in a closed glove box with nitrogen environment. D_2O and THF were contained in two separate Teflon bottles. The gas phase above the liquid phase was periodically flushed with nitrogen gas and the bottles were periodically shaken to facilitate the diffusion of oxygen out of the liquid phase. After the gas phase had been flushed six or seven times over a period of 12 h, THF and D_2O samples were accurately weighted on a precision balance from METTLER TOLEDO in a nitrogen environment and mixed on a molar basis of 1:17 in the glass bottle. This is the same concentration of THF as in the hydrate phase. Therefore, as hydrate forms, the liquid phase composition should not change. Moreover, it has been shown in interferometric studies [28] of the growth of hydrate crystals from THF/H_2O = 1/17 molar ratio solution that the THF concentration remains unchanged throughout the growth process. The sample was then sealed and moved into the Maran for measurements. It was carefully placed in the "sweet spot" of the magnet, the spot where the magnetic field is the most homogenous.

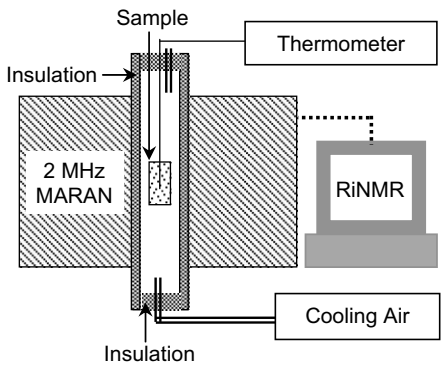

Fig. 1. Experimental schematic.

Contrary to occasional assertions in the literature that a water/THF solution is homogenous with any mixing ratios, a thorough review of the broader literature revealed that such solution is actually heterogeneous on a microscopic level and this heterogeneity has been established in many laboratories, [29–32] even for water–methanol mixture. [33] Liquid THF is in the form of small clusters dispersed in the water phase. In a recent paper [34], we reported that the proton spin lattice relaxation time (T_1) of THF in D_2O, after THF hydrate dissociation, was consistently smaller than the fresh THF–D_2O mixture before hydrate formation. Because THF and D_2O molecules are homogenously stacked in hydrate structures, it was suggested that the THF–D_2O solution became more microscopically homogenous after hydrate dissociation compared to a freshly mixed THF–D_2O solution and it could be the cause for the T_1 divergence. To ensure that the THF–D_2O solution was already homogenous and in its equilibrium configuration before hydrate formation, in this study, the freshly mixed THF–D_2O solution was first turned into hydrate and subsequently dissociated. It was warmed up to 35 °C for about 2 h to eliminate any possible remnant hydrogen bonding structure [35]. T_2 measurements were started as the sample was cooled down in steps until the point of hydrate nucleation, which was identified by the sudden rise of the sample temperature. The temperature of the cooling air was then adjusted to slow down the hydrate formation rate for better T_2 measurements. After each measurement, *WinDXP* program was executed to calculate the T_2 distribution. This program utilizes the BRD (Butler, Reeds and Dawson) algorithm [36] with zeroth order regularization to perform continuously distributed exponential fitting on the raw NMR data. The more homogenous the sample, the narrower and more symmetrical its T_2 distribution peak will be. More details can be found in the latest *WinDXP* user manual. Each experiment required about 5–10 min to complete, depending on the number of scans and the delay time between two consecutive scans. The relaxation delay time should be longer than $5T_1$ to allow the spins to fully recover before next excitation. After complete hydrate formation, marked by the disappearance of the THF liquid peak in the T_2 distribution, the sample was further cooled down to measure the T_2 behavior of THF in clathrate hydrate with regard to temperature. Then the sample was warmed up to slowly dissociate the hydrate and the temperature was subsequently raised to room temperature in steps.

3. Results and discussion

T_2 distributions of THF in D_2O during hydrate formation were presented in Fig. 2, along with the T_2 distribution before hydrate formation at the THF/D_2O hydrate equilibrium temperature ~7.5 °C, which was determined in this work. It is evident that THF in the hydrate phase and the coexisting liquid phase can be easily distinguished as two well resolved populations. The

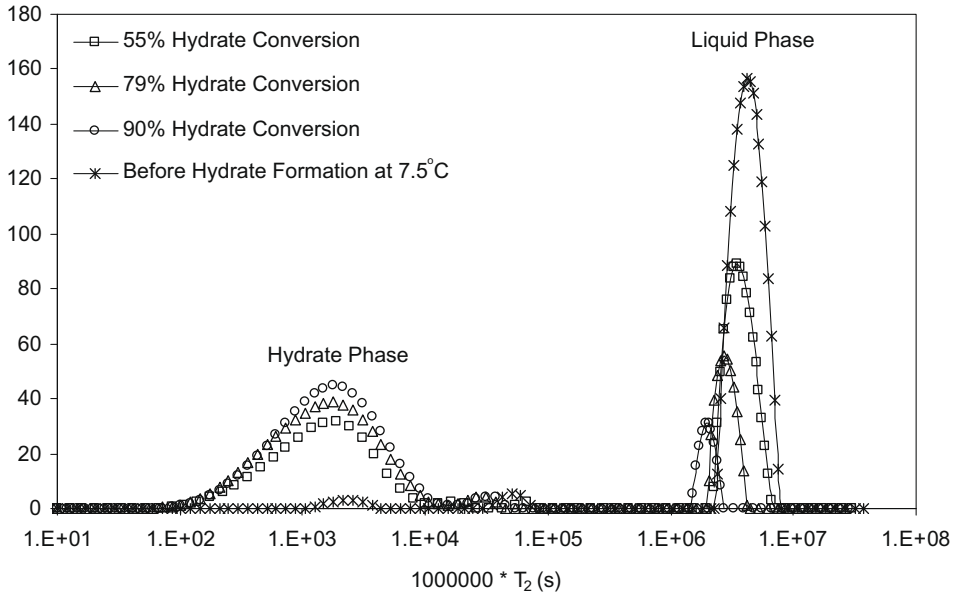

Fig. 2. T_2 distributions of THF in D_2O at different hydrate conversion percentages during hydrate formation, compared with the T_2 distribution of THF in D_2O before hydrate formation at the hydrate equilibrium temperature. *Y*-axis is dimensionless.

T_2 of THF in the hydrate phase centers around ~ 2–3 ms, but its distribution is broad and spans two orders of magnitude, which is in agreement with the observation of THF behavior in the hydrate phase reported by Garg et al. [25]. T_2 of THF in the liquid phase changed from 4.2 to 3.5 to 2.0 s as the percentage of hydrate in the sample increased from 0% to 55% to 90%. The accuracy of the T_2 data in this work is ±3.07%. The liquid THF signal disappeared after complete hydrate formation, leaving only the NMR response from THF in the hydrate phase, which confirmed the good stoichiometric control of the THF/D_2O solution. The temperature across the sample was uniform at the hydrate equilibrium temperatures, as confirmed by temperature readings at various sample spots. As shown in Fig. 3, during hydrate formation, the hydrate peak area increased while the liquid peak area decreased. The sum of hydrate and liquid peak areas was conserved. This confirmed the technique's ability of fully capturing THF molecules in the hydrate cages. In Fig. 2, there was often a small fraction of THF population between THF in the liquid phase and in hydrate phase, indicating a possible intermediate structural state. This phenomenon has not been thoroughly understood.

The dependence of $\ln(1/T_2)$ on $1/T$ (T is temperature in K) during cooling, hydrate formation, hydrate dissociation, and warming up, was plotted in Fig. 4. Garg et al. [25] concluded that THF molecules undergo extremely fast isotropic rotations in D_2O clathrate cages when the temperature is higher than 250 K. Therefore, under the conditions of interest in this work, THF proton spins in both the solid and liquid phases should relax by mainly the same intra-dipole–dipole interaction mechanism [34]. According to NMR theory [37], the rotational activation E_a can be calculated from the slope of $\ln(1/T_2) \sim 1/T$ if the rotational motion is in the extreme narrowing region and Arrhenius equation $\tau_c = \tau_o \exp(E_a/RT)$ is assumed. In this equation, R is the universal gas constant; τ_c—re-orientational correlation time; τ_o—time constant at infinite temperature; E_a is a measure of local molecular ordering around the NMR responding molecules. The $\ln(1/T_2)$~$1/T$ relationship changed its slope during cooling. The data could be fitted into two different linear regions with each R-squared value better than 0.99. This slope deviation [15] during the cooling process was observed previously. The deviation point was located 1–2 °C above the hydrate equilibrium temperature. This deviation suggested that the molecular environment around the THF molecules in the liquid phase changed as the temperature was decreased below the hydrate equilibrium point. The detailed mechanism is still to be understood.

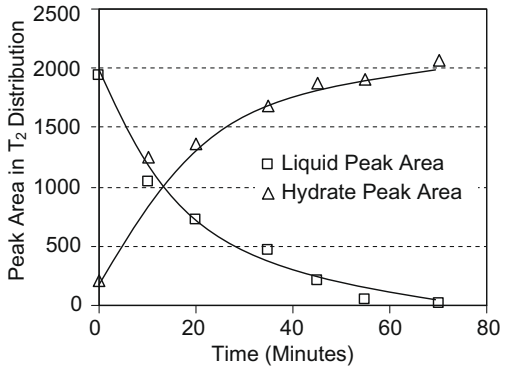

Fig. 3. Peak areas of THF in liquid phase and hydrate phase during hydrate formation as a function of time. Lines were added to guide the eyes.

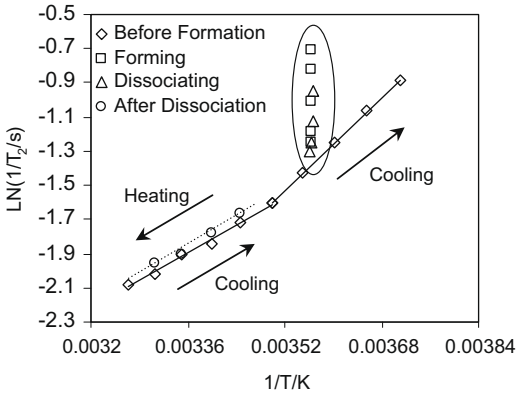

Fig. 4. T_2 behaviors of THF in D_2O solution at different temperatures and conditions.

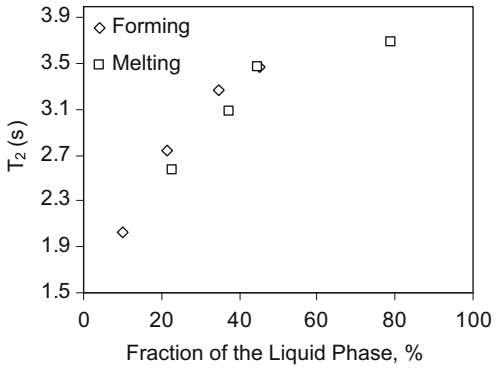

Fig. 5. T_2 of THF in D_2O solution as a function of the liquid phase fraction during hydrate formation and dissociation.

Our earlier work [27] reported that T_1 (measured at 85 MHz) of liquid THF in D_2O during hydrate transition varied as hydrate formation or dissociation progressed. This implies the fluid structure during hydrate transition was different from the fluid structure in which hydrate was not present. T_2 (measured with a 2 MHz magnet) results from this work also changed with the progress of hydrate transition at constant temperature. Fig. 5 presented the T_2 of THF in D_2O solution as a function of the liquid phase fraction during hydrate transition—the less the liquid, the shorter the T_2. The combined observation of longer T_1 [34] and shorter T_2 in the bulk liquid phase during hydrate phase transition strongly supports the proposition that the presence of a hydrate phase influences the hydrogen bonding network of the coexisting liquid phase. Hydrate transition was held at certain solid-to-liquid ratios for many hours. No T_2 change with time was observed, which suggested that this hydrate influence on the liquid structure was not transient but stable. T_2 during melting was slightly shorter than T_2 during forming (Fig. 5), but the difference was too small to yield a definitive trend.

T_2's of THF in the hydrate phase were measured in the temperature range of ~260–275 K, plotted as $\ln(1/T_2/\text{ms})$–$1/T$/K in Fig. 6. Combined with the Arrhenius equation $\tau_c = \tau_o \exp(E_a/RT)$ the slope of $\ln(1/T_2/\text{ms})$–$1/T$/K yielded an activation energy of 31 KJ/mol. Considering that the temperature range in this work was limited, this value fortuitously agreed with the activation energy given by Garg et al. [25], ~30 KJ/mol, and the value reported by Hayward and Packer [38], 33 KJ/mol. Garg et al. [25] assigned this value to the motion of D_2O in the clathrate lattice.

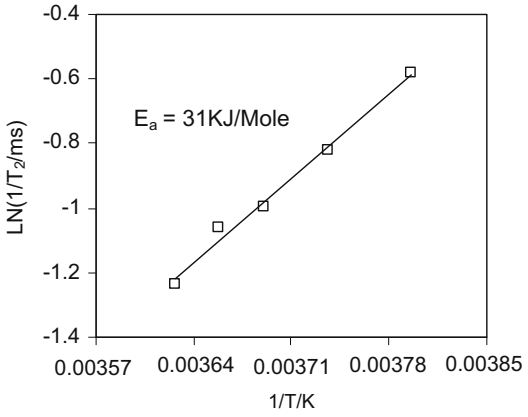

Fig. 6. T_2 of THF in D_2O clathrate cages in the temperature range of 260–275 K, plotted as $\ln(1/T_2/\text{ms})$ vs. $1/T$/K.

4. Conclusions

T_2 of THF in D_2O clathrate cages was obtained by the low field NMR T_2 distribution measurements, which gave a mean value about 2 ms at ~7.5 °C. It was demonstrated that the T_2 distribution technique is a valuable tool for investigating clathrate hydrate mechanisms. It is capable of obtaining dynamic molecular information of both hydrate phase and the coexisting liquid phase simultaneously during hydrate transition. Due to its ability of directly measuring the extent of hydrate conversion in a timely manner, extension of this technique can be potentially applied to gather hydrate kinetic data.

As temperature decreased from higher to lower regions, the slope $\ln(1/T_2)$–$1/T$ shifted to a larger value, indicating the motion of THF molecules underwent a certain transformation. T_2 of THF in D_2O solution decreased as hydrate formation progressed. Combined with previous observation that T_1 became longer during hydrate phase transition, this shortening of T_2 confirms that the fluid structure changed as more hydrate was present. The activation energy measured from the proton response of THF in hydrate phase was calculated to be 31 KJ/mol in the temperature range 260–275 K, which agreed with the values reported in the literature.

Acknowledgment

We thank the Robert A. Welch Foundation (Grant C-1241) and the Livermore Chair (TTU) for financial support.

References

[1] E.D. Sloan, Clathrate Hydrates of Natural Gases, second ed., Marcel Dekker, New York, 1998.
[2] E.D. Sloan, Hydrate Engineering, Society of Petroleum Engineers, 2000.
[3] G.R. Dickens, J.R. O'Neil, D.K. Rea, R.M. Owen, Dissociation of oceanic methane hydrate as a cause of the carbon isotope excursion at the end of the paleocene, Paleoceanography 10 (1995) 965–971.
[4] R.A. Kerr, Gas hydrate resource: smaller but sooner, Science 303 (2004) 946–947.
[5] C.A. Koh, Towards a fundamental understanding of natural gas hydrates, Chem. Soc. Rev. 31 (2002) 157–167.
[6] C.A. Koh, J.L. Savidge, C.C. Tang, Time-resolved in-situ experiments on the crystallization of natural gas hydrates, J. Phys. Chem. 100 (1996) 6412–6414.
[7] C.A. Koh, R.E. Westacott, W. Zhang, K. Hirachand, J.L. Creek, A.K. Soper, Mechanisms of gas hydrate formation and inhibition, Fluid Phase Equilibr. 194–197 (2002) 143–151.
[8] S. Hirai, K. Okazaki, Y. Tabe, K. Kawamura, CO_2 clathrate–hydrate formation and its mechanism by molecular dynamics, Energy Convers. Manage. 38 (Suppl) (1997) S301–S306.
[9] G.J. Guo, Y.G. Zhang, Y.J. Zhao, K. Refson, G.H. Shan, Lifetimes of cage-like water clusters immersed in bulk liquid water: a molecular dynamics study on gas hydrate nucleation mechanisms, J. Chem. Phys. 121 (2004) 1542–1547.
[10] J.M. Herri, J.S. Pic, F. Gruy, M. Cournil, Methane hydrate crystallization mechanism from in-situ particle sizing, AIChE J. 45 (1999) 590–602.
[11] K. Lekvam, P. Ruoff, Kinetics and mechanism of methane hydrate formation and decomposition in liquid water. Description of hysteresis, J. Cryst. Growth 179 (1997) 618–624.
[12] Y.H. Mori, T. Mochizuki, Dissolution of liquid CO_2 into water at high pressures: a search for the mechanism of dissolution being retarded through hydrate–film formation, Energy Convers. Manage. 39 (1998) 567–578.
[13] E.D. Sloan Jr., F. Fleyfel, A molecular mechanism for gas hydrate nucleation from ice, AIChE J. 37 (1991) 1281–1292.
[14] T. Uchida, A. Takagi, S. Mae, J. Kawabata, Dissolution mechanisms of CO_2 molecules in water containing CO_2 hydrates, Energy Convers. Manag0065. 38 (1997) 307–312.
[15] G.J. Guo, Y.G. Zhang, H. Liu, Effect of methane adsorption on the lifetime of a dodecahedral water cluster immersed in liquid water: a molecular dynamics study on the hydrate nucleation mechanisms, J. Phys. Chem. 111 (2007) 2595–2606.
[16] T. Pietrass, H.C. Gaede, A. Bifone, A. Pines, J.A. Ripmeester, Monitoring xenon clathrate hydrate formation on ice surfaces with optically enhanced ^{129}Xe NMR, J. Am. Chem. Soc. 117 (1995) 7520–7525.
[17] I.L. Moudrakovski, A.A. Sanchez, C.I. Ratcliffe, J.A. Ripmeester, Nucleation and growth of hydrates on ice surfaces: new insights from ^{129}Xe NMR experiments with hyperpolarized xenon", J. Phys. Chem. B 105 (2001) 12338–12347.
[18] A. Gupta, S.F. Dec, C.A. Koh, E.D. Sloan Jr., NMR investigation of methane hydrate dissociation, J. Phys. Chem. C 111 (2007) 2341–2346.

[19] G.J. Hirasaki, S.W. Lo, Y. Zhang, NMR properties of petroleum reservoir fluids, Magn. Reson. Imaging 21 (2003) 269–277.
[20] M. Bach-Verge, S.J. Kitchin, K.D.M. Harris, M. Zugic, C.A. Koh, Dynamic properties of the tetrahydrofuran clathrate hydrate, investigated by solid state ^{2}H NMR spectroscopy, J. Phys. Chem. B 105 (2001) 2699–2706.
[21] T.M. Kirschgen, M.D. Zeidler, F. Fujara, A deuteron NMR study of the tetrahydrofuran clathrate hydrate—part I: relaxation pathways, Phys. Chem. Chem. Phys. 5 (2003) 5243–5246.
[22] T.M. Kirschgen, M.D. Zeidler, F. Fujara, A deuteron NMR study of the tetrahydrofuran clathrate hydrate—part II: coupling of rotational and translational dynamics of water, Phys. Chem. Chem. Phys. 5 (2003) 5247–5252.
[23] Y.T. Seo, H. Lee, Structure and guest distribution of the mixed carbon dioxide and nitrogen hydrates as revealed by X-ray diffraction and ^{13}C NMR spectroscopy, J. Phys. Chem. B 108 (2004) 530–534.
[24] R.L. Kleinberg, C. Flaum, C. Straley, P.G. Brewer, G.E. Malby, E.T. Peltzer III, G. Friederich, J.P. Yesinowski, Seafloor nuclear magnetic resonance assay of methane hydrate in sediment and rock, J. Geophys. Res. 108 (2003) 2137.
[25] S.K. Garg, D.W. Davidson, J.A. Ripmeester, NMR behavior of the clathrate hydrate of tetrahydrofuran I. Proton measurements, J. Magn. Reson. 15 (1974) 295–309.
[26] S. Devarakonda, A. Groysman, A.S. Myerson, THF–water hydrate crystallization: an experimental investigation, J. Cryst. Growth 204 (1999) 525–538.
[27] S. Gao, W. House, W.G. Chapman, NMR/MRI study of clathrate hydrate mechanisms, J. Phys. Chem. B 109 (2005) 19090–19093.
[28] K. Nagashima, Y. Yamamotob, M. Takahashi, T. Komai, Interferometric observation of mass transport processes adjacent to tetrahydrofuran clathrate hydrates under non equilibrium conditions, Fluid Phase Equilibr. 214 (2003) 11–24.
[29] T. Fukasawa, Y. Tominaga, A. Wakisaka, Molecular association in binary mixtures of tert-butyl-alcohol water mixtures and tetrahyrofuran–heavy water studied by mass spectrometry of clusters from liquid droplets, J. Phys. Chem. A 108 (2004) 59–63.
[30] T. Takamuku, A. Nakamizo, M. Tabata, K. Yoshida, T. Yamaguchi, T. Otomo, Large-angle X-ray scattering, small-angle neutron scattering, and NMR relaxation studies on mixing states of 1,4-dioxane-water, 1,3-dioxane-water, and tetrahydrofuran–water mixtures, J. Mol. Liquid 103-104 (2003) 143–159.
[31] C.M. Sorensen, Dynamic light scattering study of tetrahydrofuran and water solutions, J. Phys. Chem. 92 (1988) 2367–2370.
[32] G. Atkinson, S. Rajagopalan, B.L. Atkinson, Ultrasonic absorption of aqueous binary mixtures 3. Tetrahydrofuran–water at 25 °C, J. Phys. Chem. 85 (1981) 733–739.
[33] J.H. Guo, Y. Luo, A. Augustsson1, S. Kashtanov, J.E. Rubensson, D.K. Shuh, H. Ågren, J. Nordgren, Molecular structure of alcohol–water mixtures, Phys. Rev. Lett. 91 (2003) 157401–157404.
[34] S. Gao, W. House, W.G. Chapman, NMR and viscosity investigation of clathrate hydrate formation and dissociation, Ind. Eng. Chem. Res. 44 (2005) 7373–7379.
[35] P. Buchanan, A.K. Soper, H. Thompson, R.E. Westacott, J.L. Creek, G. Hobson, C.A. Koh, Search for memory effects in methane hydrate: structure of water before hydrate formation and after hydrate decomposition, J. Chem. Phys. 123 (2005) 164507.
[36] J.P. Butler, J.A. Reeds, S.V. Dawson, Estimating solutions of first kind integral equations with nonnegative constraints and optimal smoothing, SIAM J. Numer. Anal. 18 (1981) 381–397.
[37] E. Fukushima, S.B.W. Roeder, Experimental Pulse NMR—A Nuts and Bolts Approach, Westview Press, 1981.
[38] R.J. Hayward, K.J. Packer, Proton magnetic relaxation in ethylene oxide, tetrahydrofuran, and triethylene diamine as clathrate deuterates, Mol. Phys. 25 (1973) 1443–1450.